Cladding defects in hollow core fibers for surface mode suppression and improved birefringence

Michieletto, Mattia; Lyngso, J. K.; Lægsgaard, Jesper; Bang, Ole

Published in:
Optics Express

Link to article, DOI:
10.1364/OE.22.023324

Publication date:
2014

Document Version
Publisher's PDF, also known as Version of record

Cladding defects in hollow core fibers for surface mode suppression and improved birefringence

M. Michieletto,[1,2,*] **J. K. Lyngsø,**[1] **J. Lægsgaardø,**[1,2] **and O. Bang**[1,2]

[1] *NKT Photonics A/S - Blokken 84 - DK-3460 Birkerd, Denmark*
[2] *DTU Fotonik, Ørsteds Plads, bygning 343, 2800 Kgs Lyngby, Denmark*
[*] *mmi@nktphotonics.com*

Abstract: We demonstrate a novel polarization maintaining hollow-core photonic bandgap fiber geometry that reduces the impact of surface modes on fiber transmission. The cladding structure is modified with a row of partially collapsed holes to strip away unwanted surface modes. A theoretical investigation of the surface mode stripping is presented and compared to the measured performance of four 7-cells core fibers that were drawn with different collapse ratio of the defects. The varying pressure along the defect row in the cladding during drawing introduces an ellipticity of the core. This, combined with the presence of antiresonant features on the core wall, makes the fibers birefringent, with excellent polarization maintaining properties.

OCIS codes: (060.2280) Fiber design and fabrication; (060.5295) Photonic crystal fibers; (060.2420) Fibers, polarization-maintaining.

References and links

1. M. Digonnet, S. Blin, H. K. Kim, V. Dangui, and G. Kino, "Sensitivity and stability of an air-core fibre-optic gyroscope," Meas. Sci. Technol. **18**(10), 3089 (2007).
2. J. Hald, J. C. Petersen, and J. Henningsen, "Saturated optical absorption by slow molecules in hollow-core photonic band-gap fibers," Phys. Rev. Lett. **98**(21), 213902 (2007).
3. A. D. Slepkov, A. R. Bhagwat, V. Venkataraman, P. Londero, and A. L. Gaeta, "Spectroscopy of Rb atoms in hollow-core fibers," Phys. Rev. A **81**(5), 053825 (2010).
4. R. Amezcua-Correa, N. G. Broderick, M. N. Petrovich, F. Poletti, and D. J. Richardson, "Optimizing the usable bandwidth and loss through core design in realistic hollow-core photonic bandgap fibers," Opt. Express **14**(17), 7974–7985 (2006).
5. P. J. Roberts, D. P. Williams, H. Sabert, B. J. Mangan, D. M. Bird, T. A. Birks, and P. St. J. Russell, "Design of low-loss and highly birefringent hollow-core photonic crystal fiber," Opt. Express **14**(16), 7329–7341 (2006).
6. P. J. Roberts, F. Couny, H. Sabert, B. J. Mangan, D. P. Williams, L. Farr, and P. St. J. Russell, "Ultimate low loss of hollow-core photonic crystal fibres," Opt. Express, **13**(1) 236–244 (2005).
7. C. I. Falk, J. Hald, J. C. Petersen, and J. K. Lyngsø, "Transmission properties of hollow-core photonic bandgap fibers in relation to molecular spectroscopy," Appl. Opt. **49**(20), 3854–3859 (2010).
8. J. K. Lyngsø, C. Jakobsen, H. R. Simonsen, and J. Broeng, "Single-mode 7-cell core hollow core photonic crystal fiber with increased bandwidth," Proc. SPIE 7753, 77533Q (2011)
9. E. N. Fokoua, M. N. Petrovich, N. K. Baddela, N. V. Wheeler, J. R. Hayes, F. Poletti, and D. J. Richardson, "Real-time prediction of structural and optical properties of hollow-core photonic bandgap fibers during fabrication," Opt. Lett. **38**(9), 1382–1384 (2013).
10. F. Couny, F. Benabid, P. J. Roberts, M. T. Burnett, and S. A. Maier, "Identification of Bloch-modes in hollow-core photonic crystal fiber cladding," Opt. Express **15**(2), 325–338 (2007).
11. F. Poletti and E. N. Fokoua, "Understanding the physical origin of surface modes and practical rules for their suppression," in Proceedings of IEEE The 39th European Conference and Exhibition on Optical Communication (IEEE, 2013), pp. 1–3.

#212845 - $15.00 USD Received 12 Jun 2014; revised 31 Jul 2014; accepted 7 Aug 2014; published 16 Sep 2014

12. G. Kim, K. Hwang, K. Lee, K. S. Lee, Y. G. Han, and S. B. Lee, "Experimental study of an elliptical-core photonic bandgap fiber with thin core wall and high aspect ratio and its birefringence characteristics," Appl. Phys. B **101**(3), 583–586 (2010).
13. X. Chen, M. J. Li, N. Venkataraman, M. Gallagher, W. Wood, A. Crowley, and K. Koch, "Highly birefringent hollow-core photonic bandgap fiber," Opt. Express **12**(16), 3888–3893 (2004).
14. F. Poletti, N. G. Broderick, D. Richardson, and T. Monro, "The effect of core asymmetries on the polarization properties of hollow core photonic bandgap fibers," Opt. Express **13**(22), 9115–9124 (2005).
15. R. Calvani, R. Caponi, and F. Cisternino, "Polarization measurements on single-mode fibers," J. Lightwave Technol. **7**(8), 1187–1196 (1989).

1. Introduction

Hollow core photonic band gap (HC-PBG) fibers have been employed for high precision sensors, e.g. fiber optic gyroscopes and gas spectroscopy [1, 2]. Even though they offer unique properties, like very high optical depth [3] and low non-linearity, they also show some limitations. One of the drawbacks of HC-PBG is the presence of surface modes (SMs), i.e. supported modes which have a field distribution localized on the core wall. It has been shown that with a careful design of the core-wall, and in particular of its thickness [4], anti-crossing events of these modes with the fundamental mode (FM) can be placed outside the band-gap to increase as much as possible the operative bandwidth of HC-PBG fibers. This principle has been used in the past to obtain surface mode free HC-PBG fiber. In many applications though, as the ones mentioned above, it is important for the fiber to be polarization maintaining. A well-known technique to get a polarization maintaining HC-PBG fiber relies on the introduction of anti-resonant features on the core wall [5]. These features set a constrain on the core wall design, and they modify the location of surfaces modes within the bandgap. This complication makes it unlikely to achieve surface modes free fibers solely through a specific core wall design in the case of polarization maintaining fiber and it means that SMs will be present within the bandgap. Surface roughness scattering, which is the main contributor to loss in HC-PBG fibers [6], facilitates the coupling between the fundamental mode and the surface modes. Therefore even in spectral regions far from anti-crossing events light can scatter out of the fundamental mode into surface modes along propagation. In many applications this issue limits the performance since it affects the transmission stability over time [7]. The fiber is multi-mode because of the presence of surface modes and geometrical deformation of the fiber due to thermal variations, vibrations or bending induces transmission instabilities. In this work we show that it is possible through the introduction of controlled defects in the cladding structure to strip away surface modes at a given wavelength, hence reducing their effect on the transmission. Moreover the defects can be exploited to enhance the fiber polarization holding. Indeed placing them along a row in the cladding allows an elliptical core to be obtained. These improvements though come to the detriment of bandwidth and loss. We have measured a low coupling between the polarization states of the fiber characterized by an h-parameter as low as $5 \times 10^{-5}\mathrm{m}^{-1}$. This together with the low loss (about 60dB/km at 1550nm) make this fiber design a candidate for many applications where low loss, good polarization maintenance and transmission stability are needed.

2. Fibers geometry

The four 7-cell HC-PBG fibers in Fig.1 were fabricated using the stack and draw technique. The fibers were drawn from the same preform. The capillaries that correspond to the cladding defects have pressure control independent from the rest of the cladding, which allow to introduce a pressure difference during drawing that was used to produce the cladding defects in a controlled way.

In order to investigate and understand the resonant coupling between surface modes and cladding defects we developed a model based on an idealized geometry. The starting point is

#212845 - $15.00 USD Received 12 Jun 2014; revised 31 Jul 2014; accepted 7 Aug 2014; published 16 Sep 2014

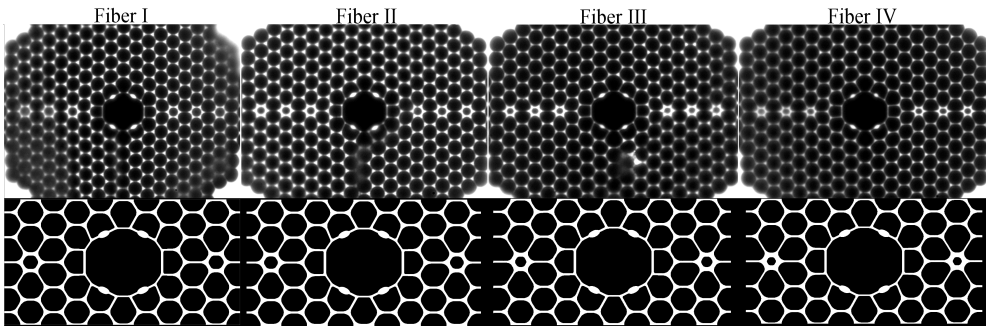

Fig. 1. Top:Microscope images of the fibers considered. Bottom: Corresponding idealized structures used in the modeling.

a standard realistic geometry for HC-PBG fibers [8]. The deformations we need to reproduce in our model are the partially collapsed holes in the cladding and the ellipticity of the fiber. In order to achieve that, the following assumptions were made. The glass area of the fiber is a conserved quantity, the portion of the cladding without the defects is still a regular hexagonal lattice, and there is no glass flow between apex and strut or between different unit cells. The total glass area conservation is a requirement given by the manufacturing technique. The local area conservation in each unit cell, strut and apex has been proven to be a good approach in previous publications [9]. The weaker assumption is the one about the preserved regularity in the cladding lattice since the microscope images indicate that this is not completely true, especially for the outer cladding rings. If we define the collapse ratio α as the ratio between the diameter of the hole in the defect and the unaltered average cladding hole diameter the four fibers considered has the following collapse ratios $\alpha_I = 60\%$ $\alpha_{II} = 55\%$ $\alpha_{III} = 46\%$ $\alpha_{IV} = 37\%$. The four fibers have the same pitch of 3.2µm, the same apex radius of curvature of 1.06 µm, the same strut thickness of 180nm and the same core ellipticity with an aspect ratio of about 1.2.

A first set of simulations were done with only four rings (one defect per core side) for the four geometries to illustrate how the cladding defect modes localize within the bandgap and how they are affected by the different collapse ratios.

A further analysis were done with six and eight rings of holes (two and three defects per core side, respectively) to investigate the effect of multiple cladding defects. This was done only for the geometry that offers the best performance (Fiber III).

3. Surface mode stripping

The aim of the proposed method is to attenuate unwanted surface modes by resonantly coupling with a high loss cladding defect mode. Ideally the attenuation of the surface mode does not affect the fundamental core mode at a given wavelength (1550 nm in the current work). This situation is depicted in Fig.2. The mode field distributions show that at a given wavelength, with the introduction of cladding defects, is possible to have surface mode stripping. At a longer wavelength couplings between the cladding defect mode and the fundamental modes occur.

Let us now focus on the simulations in Fig.3 regarding the four fibers that were drawn. The different colors correspond to different kind of modes: blue dots correspond to modes that localize on the cladding defects, green dots are surface modes and red dots are the fundamental core guided modes. We can distinguish two different kinds of cladding defect modes. In fiber I and II only ”apex”-like modes [10, 11] are present, they enter the bandgap from the long wavelength edge and then shift towards shorter wavelength as the collapse ratio decreases, moreover they show a dispersion similar to that of the surface modes. In fiber III and IV also

#212845 - $15.00 USD Received 12 Jun 2014; revised 31 Jul 2014; accepted 7 Aug 2014; published 16 Sep 2014

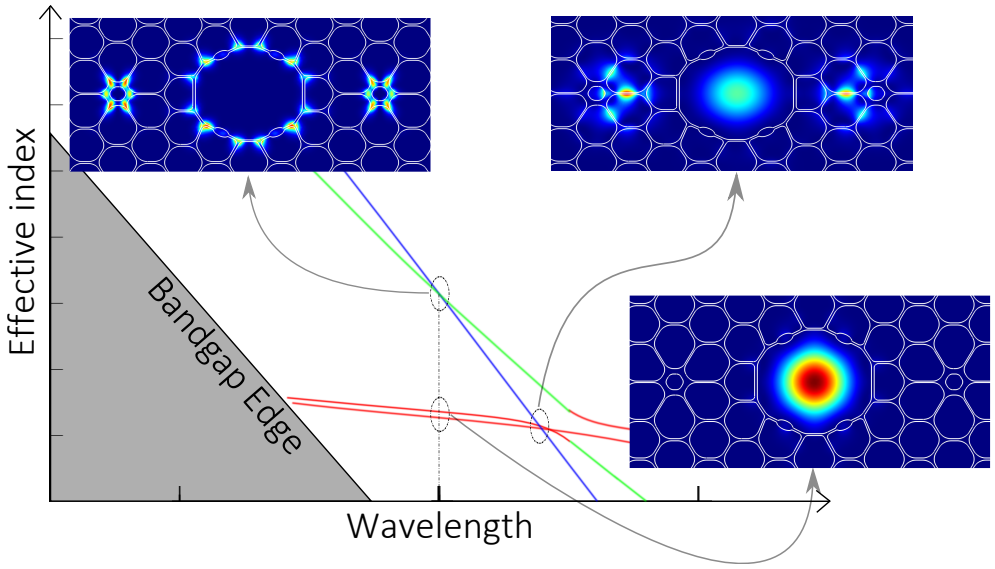

Fig. 2. Sketch of the surface mode stripping. The green line represents an unwanted surface mode, the red lines the two polarization of the fundamental mode and the blue line is the cladding defect mode that can be used to attenuate the surface modes

”airy”-like [10, 11] modes enter the bandgap from the lower edge.

The fiber trasmission measurements obtained using a supercontinuum source through butt coupling the FUT to a single mode fiber and recording with an OSA are also shown in Fig.3. Comparing these measurements with the simulated mode trajectories we note there is a good agreement for the behaviour of the fundamental mode, especially regarding the operational bandwidth around 1550nm. We believe that the mismatch at longer wavelengths is due to the fact that the simulation is limited to only four rings of holes (one defect per core side).

This analysis shows how the collapse ratio play an essential role and it allows to place the cladding defect modes where needed across the bandgap.

The four rings geometry though does not capture the whole picture. To illustrate the effect of multiple defects per core side we therefore performed simulations also for six and eight rings cladding fibers. The geometry of Fiber III has been used for these simulations.

As it is possible to see in Fig.4 surface modes do not change with the number of rings considered, as expected, since the core wall geometry is unaltered. The band edge of the simulated fibers approach the one predicted by the simulation for an infinite cladding structure as the number of rings increase. We believe that this effect is due to the fact that with a small number of rings the finite extent of the photonic crystal cladding reduces the number of cladding modes and thereby increase the bandgap compared to what one would expect from an infinite crystal.

What is more relevant for this work is that the cladding defect modes split due to the establishment of supermodes, increasing the possibility of crossing between cladding defect modes and surface modes. Because of the complexity of the dispersion figures we estimated the couplings between all the defect modes and all the surface modes in order to clarify which crossings are relevant. Since these modes have a considerable field amplitude at the glass/air interfaces we considered scattering from glass surface roughness as a primary contribution to the couplings. For this reason, similarly to what is typically done to estimate scattering loss for the

#212845 - $15.00 USD Received 12 Jun 2014; revised 31 Jul 2014; accepted 7 Aug 2014; published 16 Sep 2014

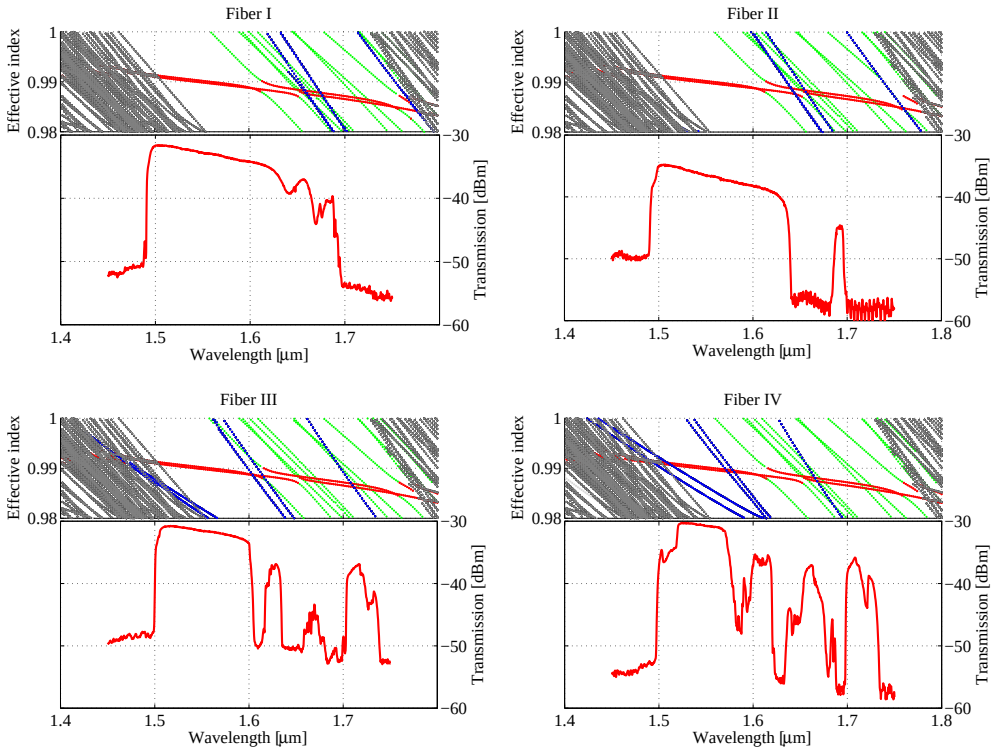

Fig. 3. For the four fibers the simulations from the idealized model (upper part of each quadrant) and the measured transmissions over 1 meter fiber (bottom part of each quadrant) are compared. In the mode trajectory plots green dots represent surface modes, red dots the fundamental modes, blue dots the cladding defect modes and dark grey the cladding modes

fundamental mode [6], we define the following overlap integral as coupling coefficient:

$$\eta = \frac{\left| \oint_{\text{glass/air interfaces}} \mathbf{E}_1^* \cdot \mathbf{E}_2 \, \mathrm{d}l \right|^2}{\int (\mathbf{E}_1 \times \mathbf{H}_1^*) \cdot \hat{\mathbf{z}} \, \mathrm{d}A \int (\mathbf{E}_2 \times \mathbf{H}_2^*) \cdot \hat{\mathbf{z}} \, \mathrm{d}A} \tag{1}$$

The simulations were performed in a quarter domain for all the four boundary conditions, therefore η was evaluated only between modes calculated with the same boundary conditions, since otherwise it would automatically be zero for symmetry reasons. In Fig.4 the calculated coupling coefficients are plotted. We notice that despite the high number of crossings that are occurring only a few are relevant. Moreover since the dispersion curves of the cladding defect modes and surface modes are so similar, tiny differences in their relative location can drastically change the coupling between them, as it is evident comparing the six and eight rings cases. We also expect that more couplings than the ones predicted by the numerical model are present in a real fiber because of geometrical deformations along the fiber. A final consideration for this section is that the occurrence of supermodes, in the case of multiple defects per core side, generate more crossings between the cladding defect modes and the fundamental mode. This feature might explain the complex transmission spectra measured in fiber III and IV (see Fig.3) for wavelengths longer then 1.6µm.

#212845 - $15.00 USD Received 12 Jun 2014; revised 31 Jul 2014; accepted 7 Aug 2014; published 16 Sep 2014

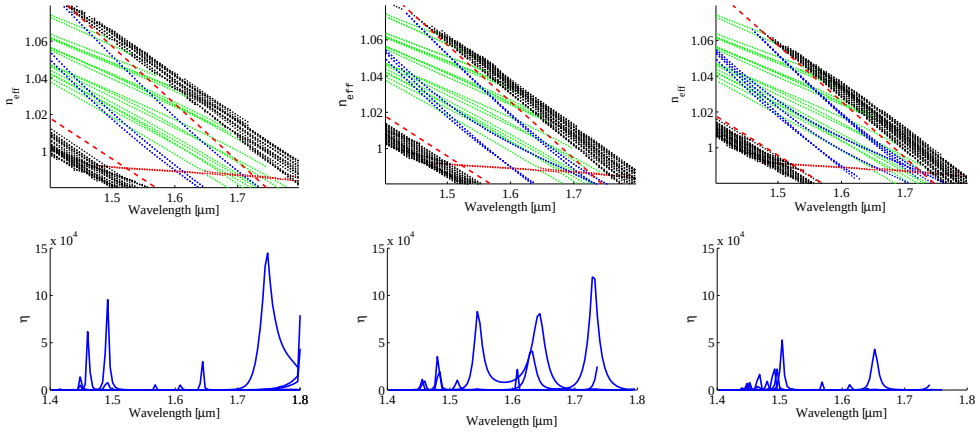

Fig. 4. The simulated mode trajectories for fiber III and the overlap integrals between surface modes and cladding defect modes are plotted in the case of 4, 6 and 8 rings of holes, respectively. Green dots represent surface modes, red dots the fundamental modes, blue dots the cladding defect modes and black dots the cladding modes. The red dashed lines represent the bandgap edges for the simulation in the case of an infinite photonic crystal

4. Characterization

In this section we present an experimental characterization of fiber III. As shown above the control on the collapse ratio allows the cladding defect modes to be shifted to a given location in the badgap. The surface mode stripping only occurs for a limited range of wavelengths, and it depends on the cladding defect modes. Depending on the wavelengths of interest any of the four fibers can be of interest. Fiber III offers the best performance at 1550nm in terms of operational bandwidth and surface mode stripping.

4.1. Surface modes stripping

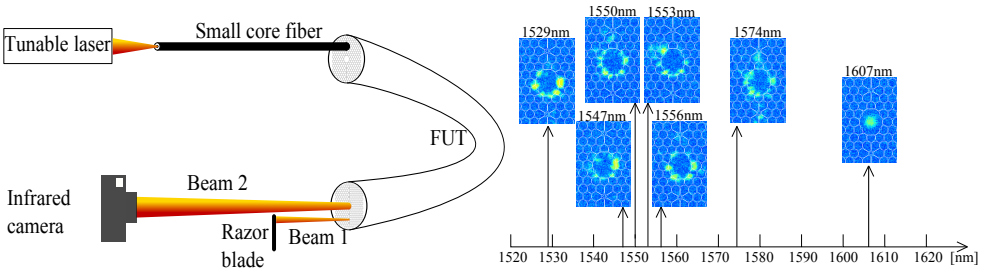

Fig. 5. (left) Schematic of the measurement, (right) Obtained optical intensity profiles

Proving experimentally the existence of coupling between cladding defect modes and surface modes as it was described so far is a challenging task. The main issues are the very lossy nature of the modes we want to characterize and the poor coupling that we could achieve to these modes. At 1550nm the simulated confinement losses for surface modes and fundamental mode are about 10dB/km and 1dB/km respectively. Their loss is then expected to be dominated by scattering losses [6]. On the other hand the confinement loss for cladding defect modes is

#212845 - $15.00 USD Received 12 Jun 2014; revised 31 Jul 2014; accepted 7 Aug 2014; published 16 Sep 2014

several thousands dB/km. Coupling light exclusively to surface modes is almost impossible with a gaussian input beam since it is inevitable to excite also some core modes, particularly the fundamental one, that would dominate in the transmission. What has proven to be a reliable method is to couple light into one of the cladding defects and look at which wavelengths coupling occurs, i.e. at which wavelengths light appears in the core area.

Fig. 5 shows a schematic of the measurement. We coupled the light of a tunable laser to a small core single mode fiber with a mode field diameter of $\sim 3\mu m$, that is about the size of the fiber pitch. Through butt coupling to the FUT we aligned the output field to the central defect on one of the core sides, in this way only cladding defect modes are excited. The output of the FUT was imaged on a infrared camera using a x40 microscope objective, the beam was spatially filtered with the use of a razor blade to exclude the residual light in the cladding defect modes, in order to image only the light in the core surround. The output signal was very weak and forced us to set the camera to maximum sensitivity and gain in order to collect the light distibution. We believe that this due to the very poor coupling between the gaussian beam from the small core fiber and the cladding defect modes.

Nevertheless we could locate three regions (see Fig.5) in which cladding defect modes clearly couple to surface modes: around 1529nm, a broader coupling in the range 1547nm $\div$1556nm and around 1574nm. Moreover, coupling to the fundamental mode was also detected at 1607nm, accordingly to what was expected from the simulation and the transmission measurement for fiber III in Fig.3. This is strong evidence that we are looking at the behaviour of at least one of the cladding defect modes described in the previous section. Outside these regions no light was detected. As expected from the numerical analysis we found the coupling to occur only on small portions of the spectrum. The discrepancy between the calculated coupling coefficients in Fig.4 and the experimental measurement in Fig.5 arise from the fact that the idealized model can not reproduce exactly the relative position of surface modes and cladding defect modes in the bandgap.

Another confirmation of the reduced amount of surface modes comes from the comparison of the near field of fiber III with a fiber that has the same cladding geometry but without any defect. Light from a tunable laser at 1550nm was coupled to a single mode fiber and the FUT was butt coupled to it. The output was imaged with a x40 microscope objective to a infrared camera. The camera used is a infrared Vidicon camera C2741 and the frames where collected with a gamma correction of 0.675 so to enhance the low intensity regions. The fibers were touched during detection to illustrate the interference between modes and thus the instabilities given by the presence of surface modes. From the movies in Fig.6 one can notice how the fiber without cladding defects (see Media 1) has more light in correspondence to the core wall and moreover in time there is a clear transfer of optical power from the core area to the core wall where surface modes are localized. This effect is highly reduced in the case of fiber III (see Media 2). Some residual light in correspondence of the core wall is expected from the fundamental mode field distribution.

4.2. Birefringence

We have designed the fiber with a 2-fold symmetric elliptical features on the core wall, that is a well known technique to make the fiber birefringent [5].

Even though HC-PBG fibers have already been produced with elliptical core, either placing the preform off-center in the furnace during drawing [12] or with a 4-cells core [13], it is the first time to our knowledge that a pressure control of some of the cladding holes is used to induce an ellipticity to the core.

A drawback of the introduction of the cladding defects is the increased loss of the fiber. The fiber in Fig.6 without cladding defects has a minimum loss of $\sim$ 20dB/km. Fiber III has a

#212845 - $15.00 USD Received 12 Jun 2014; revised 31 Jul 2014; accepted 7 Aug 2014; published 16 Sep 2014

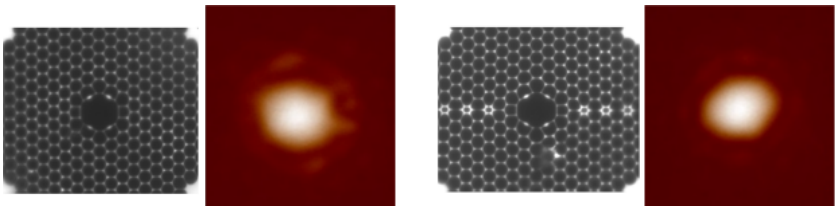

Fig. 6. Single frame from movies of the near field vs time during fiber external perturbation (touch) at 1550nm and microscope image of the fiber. Left: Fiber without cladding defects (see Media 1) Right: Fiber III (see Media 2).

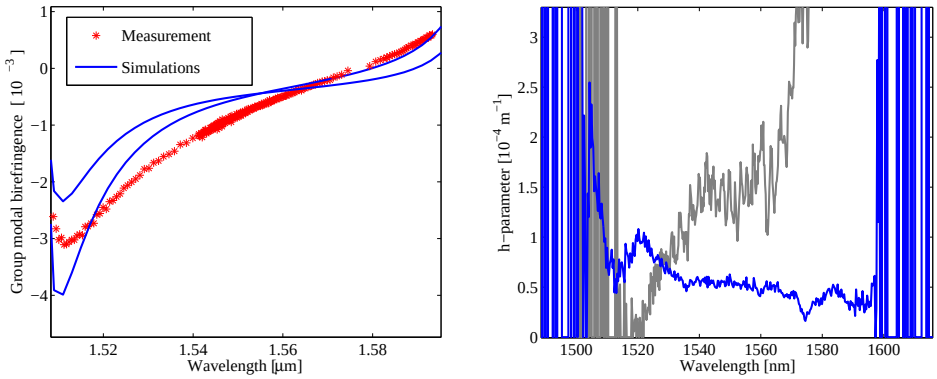

Fig. 7. Left: Measured group modal birefringence with scanning wavelength method is compared to the idealized model simulation, Right: Measured polarization holding parameter (h-parameter) in blue for fiber III and gray for a fiber with the elliptical features on the core wall, but without the cladding defects

minimum loss of $\sim$ 60dB/km and an aspect ratio of the core of 1.2. The comparison with the elliptical fiber proposed in [12], that has similar polarization properties, an aspect ratio of 1.4 and a minimum loss of $\sim$ 100dB/km, would suggest that the elliptical core is responsible to the increased loss. Nevertheless a weak coupling between the fundamental mode and the cladding defect modes can not be completely excluded.

The group modal birefringence (GMB) has been measured for fiber III by wavelength scanning method (Fig. 7) for two different fiber lengths (1.3m for the short wavelengths and 19.4m for the long wavelengths) to have a good resolution for the whole measurement range. Both polarizations of the fundamental mode were transmitted through the fiber and the interferogram was recorded. From this the absolute group birefringence was calculated by the use of

$$|B_g(\lambda)| = \frac{\lambda^2}{\Delta\lambda L} \tag{2}$$

where B_g is the group modal birefringence, L is the fiber length and $\Delta\lambda$ the wavelength spacing between two contiguous maxima on the interferogram. The sign is reconstructed from the simulation, but it is arbitrary since it depends on the birefringence given by the effective index difference. As described in [14] the group modal birefringence is highly affected by the core asymmetries and small features in the core can greatly affect it. In Fig.7 two simulations of our idealized model performed with slightly different core wall thickness are compared to the experimental measurement, showing a fairly good agreement.

#212845 - $15.00 USD Received 12 Jun 2014; revised 31 Jul 2014; accepted 7 Aug 2014; published 16 Sep 2014

GMB is not a good measure for how well the fiber maintains field polarization though. The polarization crosstalk (C) is defined [15] as the logarithmic ratio of the power P_x (P_y) coupled to the unexcited mode polarized along x (y) axis, with respect to the total transmitted power $P_x + P_y$ over a propagation length L, and it can be expressed in terms of the polarization holding parameter h:

$$C = 10\log\left(\frac{P_x}{P_x+P_y}\right) = 10\log\left(\frac{1-e^{-2hL}}{2}\right) \tag{3}$$

We estimated experimentally the h-parameter using a crossed polariser setup and the approximation [15]:

$$h \simeq \frac{2}{L(\rho_x+\rho_y)}, \quad \rho_x = \frac{P_x(L)}{P_y(L)} \quad \text{for} \quad P_y(0)=0, \quad \rho_y = \frac{P_y(L)}{P_x(L)} \quad \text{for} \quad P_x(0)=0 \tag{4}$$

where L is the length of the FUT and $P_x(l)$, $P_y(l)$ the optical powers in the two principle axis of the fiber at the given fiber length l.

Fig.7 shows the measured h-parameter for both fiber III and a fiber with the elliptical features on the core wall, but without the cladding defects(see Fig.6). Both the measurements were performed over a 50m FUT. The comparison shows that the new fiber design contribute to achieve a flat profile with a value of about 5×10^{-5} m^{-1} over a broader bandwidth around 1550nm. The minimum h-paramter for the fiber without cladding defect is located at 1520nm at the short wavelength bandgap edge. However at operative wavelengths around 1550nm it is about 15×10^{-5} m^{-1}. In the case of solid core fibers polarization holding as low as 10^{-6} m^{-1} can be achieved. If in a given application a maximum of -20dB polarization crosstalk can be tolerated, 67m of the hollow core fiber without cladding defect can be exploited, 200m in case of Fiber III and about 10km for a solid core fiber with a h-parameter of 10^{-6} m^{-1}.

5. Conclusion

A novel approach to reduce the impact of surface modes on polarization maintaining hollow core photonic band gap fibers has been proposed. The modified cladding geometry presents a row of partially collapsed holes that can be used to attenuate unwanted surface modes. The modes in the cladding defects resonantly couple with the surface modes and thus increasing their transmission loss. Four 7-cell core fibers with different collapse ratio were drawn and analyzed numerically and experimentally. There was a good agreement between the numerical analysis and experiment, which showed a significant reduction in the amount of surface modes propagating at 1550 nm. Moreover, the introduction of the cladding defects makes the core elliptical, thereby enhancing the polarization holding. An h-parameter of 5×10^{-5}m^{-1} has been measured at 1550nm, with a group modal birefringence of about 10^{-3}.

We expect this fiber design to prove its robustness in experiments in which the transmission stability, polarization maintaining and low loss are essential, such as fiber optic gyroscopes and gas saturated absorption for frequency standards.

Further improvement might also be achieved considering additional rows of defects to enhance the surface modes stripping. This approach would also allow to obtain a fiber without an elliptical core, in case this feature is unwanted.

Acknowledgments

The presented work was made possible by the Marie Curie Initial Training Network QTea, financed by the FP7 of the European Commission (contract-N MCITN-317485).